

L. Coates,<sup>a\*</sup> G. Beaven,<sup>b</sup>  
P. T. Erskine,<sup>b</sup> Samuel I. Beale,<sup>c</sup>  
S. P. Wood,<sup>b</sup> P. M. Shoolingin-  
Jordan<sup>b</sup> and J. B. Cooper<sup>b</sup>

<sup>a</sup>Bioscience Division, Los Alamos National Laboratory, Los Alamos, NM 87545, USA, <sup>b</sup>School of Biological Sciences, University of Southampton, Bassett Crescent East, Southampton SO16 7PX, England, and <sup>c</sup>Division of Biology and Medicine, Brown University, Providence, RI 02912, USA

Correspondence e-mail: lcoates@lanl.gov

## Structure of *Chlorobium vibrioforme* 5-aminolaevulinic acid dehydratase complexed with a diacid inhibitor

The structure of *Chlorobium vibrioforme* 5-aminolaevulinic acid dehydratase (ALAD) complexed with the irreversible inhibitor 4,7-dioxosebacic acid has been solved. The inhibitor binds by forming Schiff-base linkages with lysines 200 and 253 at the active site. The structure reported here provides a definition of the interactions made by both of the substrate molecules (A-side and P-side substrates) with the *C. vibrioforme* ALAD and is compared and contrasted with structures of the same inhibitor bound to *Escherichia coli* and yeast ALAD. The structure suggests why 4,7-dioxosebacic acid is a better inhibitor of the zinc-dependent ALADs than of the zinc-independent ALADs.

Received 1 July 2005

Accepted 22 September 2005

**PDB Reference:** 5-amino-  
laevulinic acid dehydratase,  
2c1h.

### 1. Introduction

The enzyme 5-aminolaevulinic acid dehydratase (ALAD, also known as porphobilinogen synthase; EC 4.2.1.24) performs its reaction at the confluence of the C-5 and Shemin pathways in tetrapyrrole biosynthesis (Jordan, 1991, 1994; Warren & Scott, 1990; Jaffe, 1995, 2000). The enzyme binds two molecules of 5-aminolaevulinic acid and condenses them to form the pyrrole porphobilinogen (Fig. 1). Four porphobilinogen molecules are then joined together and cyclized by subsequent enzymes in the pathway to form uroporphyrinogen III. The pathway diverges to produce an array of tetrapyrroles, including cobalamins, chlorophyll and haem, which are fundamental to many biological processes.

The ALAD enzymes share a high degree of sequence identity, contain about 350 amino acids per subunit and are usually octameric (Jordan, 1991, 1994; Warren & Scott, 1990; Jaffe, 1995, 2000). There are differences between the ALAD enzymes isolated from various species in terms of their metal requirements and susceptibility to oxidation (Jaffe, 2003). In humans, hereditary deficiencies in ALAD give rise to the rare

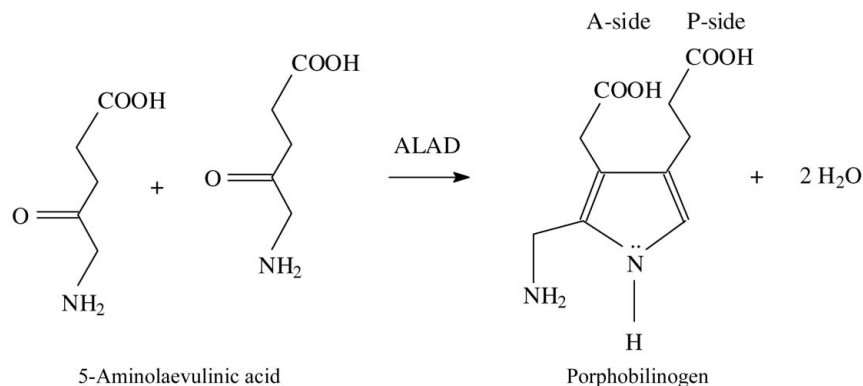


**Figure 1**

The reaction catalysed by 5-aminolaevulinic acid dehydratase (ALAD). Two molecules of 5-amino-laevulinic acid are condensed to form the pyrrole porphobilinogen.

disease Doss porphyria (Doss *et al.*, 1979) and the inhibition of the enzyme by lead ions (Simons, 1995; Jaffe *et al.*, 2001) is one of the main symptoms of acute lead poisoning (Warren *et al.*, 1998). 5-Aminolaevulinic acid structurally resembles the neurotransmitter GABA (Brennan & Cantrill, 1979) and its build-up may be responsible for some of the neurological symptoms which accompany the inhibition of ALAD in Doss porphyria and lead poisoning (Erskine *et al.*, 1997). Elevated levels of ALA are also found in the hereditary disease type I tyrosinaemia (Mitchell *et al.*, 1990), which is thought to stem from the accumulation of succinylacetone, a breakdown product of tyrosine and a potent inhibitor of ALAD.

The X-ray structures of ALAD from several sources have shown that the enzyme has a large homo-octameric structure, with each subunit adopting the ( $\beta/\alpha$ )<sub>8</sub> or TIM-barrel fold with an N-terminal arm of variable length forming intersubunit contacts (Erskine *et al.*, 1997; Erskine, Newbold *et al.*, 1999; Erskine, Norton *et al.*, 1999; Frankenberg *et al.*, 1999). Each subunit has an N-terminal arm region which allows pairs of monomers to associate with their arms wrapped around each other to form compact dimers. Four dimers, which also interact principally *via* their arm regions, form the octamer and create a large solvent-filled cavity in the centre. The active site of each subunit is located in a pronounced cavity formed by loops at the C-terminal ends of the  $\beta$ -strands forming the TIM barrel. All eight active sites are oriented towards the outer surface of the octamer and appear to be independent. Recently, evidence for hexameric quaternary forms of some ALADs has been found (Breinig *et al.*, 2003; Bollivar *et al.*, 2004).

At the base of each active site are two lysine residues (200 and 253 in *Chlorobium vibrioforme* ALAD), one of which (Lys253) is known to form a Schiff-base link to the substrate. X-ray structure analysis of most inhibitor complexes revealed that a large flap covering the active site (residues 205–225 in *C. vibrioforme* ALAD) undergoes a substantial increase in order upon formation of the Schiff base with the enzyme. In some ALADs (*e.g.* those from animal species, fungi and some bacteria) there is a well defined metal-binding site at the catalytic centre formed by three cysteine residues (133, 135 and 143 in yeast ALAD numbering) and a solvent molecule which coordinate a zinc ion (Erskine *et al.*, 1997; Jaffe, 2003). In contrast, other ALADs (typified by those from plants) lack an active-site zinc ion owing to substitution of the three cysteines at the active site with other amino acids and two such bacterial ALAD structures have been solved to date, showing that no metal ions are present at the catalytic centre (Coates *et al.*, 2004; Frankenberg *et al.*, 1999). Some ALADs of both the zinc-dependent and zinc-independent classes also possess a regulatory metal-binding site which is located between each TIM-barrel domain and the N-terminal arm of a neighbouring subunit in the octamer (Coates *et al.*, 2004; Frankenberg *et al.*, 1999; Erskine, Norton *et al.*, 1999; Kervinen *et al.*, 2001).

In the reaction catalysed by ALAD, two identical molecules of 5-aminolaevulinic acid are bonded together to form the asymmetric pyrrole product porphobilinogen. The substrate molecules (along with each of their associated binding sites)

are named according to which side of the product porphobilinogen they form, namely the acetate (A) or propionate (P) sides as shown in Fig. 1. Single turnover experiments have shown that it is the substrate molecule which goes on to constitute the propionate side of the product which binds first and it has been established that this substrate forms a Schiff base with the enzyme (Jordan & Seehra, 1980*a,b*; Jordan & Gibbs, 1985; Gibbs & Jordan, 1986). Whether it is C–N or C–C bond formation between the two substrates which finally closes the pyrrole ring is still unclear (Jaffe, 2004). Whatever the mechanism, at some point during the reaction a long-chain dicarboxylate is created as an intermediate. If C–C bond formation is first, the intermediate will take the form of a seven-carbon chain diacid, whilst if C–N bond formation occurs first a ten-atom chain diacid will be formed (Jarret *et al.*, 1998, 2000; Neier, 2000). As has been noted previously, dicarboxylic acids may be able to cross-link the carboxylic acid-binding groups associated with the A and P substrate-binding sites (Senior *et al.*, 1996; Stauffer *et al.*, 2001).

We have co-crystallized the ALAD from *C. vibrioforme* in complex with the ten-carbon-chain diacid irreversible inhibitor 4,7-dioxosebacic acid, the formula of which is shown in Fig. 2. This study shows that the inhibitor binds by forming Schiff bases at the catalytic centre with both of the invariant lysine residues (200 and 253). The finding that both invariant lysines at the active site are capable of making such an interaction without the presence of a metal ion at the active site is in accord with recent proposals for the catalytic mechanism which speculated that both the A- and P-side substrates bind by making Schiff bases with the enzyme (Erskine *et al.*, 2001, 2003). Since this inhibitor has considerably lower affinity for zinc-independent ALADs (such as the *C. vibrioforme* enzyme) than for the zinc-dependent ALADs (such as yeast and *Escherichia coli*; Kervinen *et al.*, 2001), it was of interest to determine how this molecule bound to the *C. vibrioforme* enzyme. The results of the X-ray structure analysis are presented here in comparison with the previously solved structures of this inhibitor bound to the yeast and *E. coli* enzymes (Erskine, Newbold *et al.*, 2001; Kervinen *et al.*, 2001).

## 2. Experimental

### 2.1. Data collection and data processing

Cocrystals of *C. vibrioforme* ALAD with the inhibitor were obtained using the hanging-drop method with the same conditions as those used for the native enzyme (Coates *et al.*, 2004), except for addition of the inhibitor to give a final concentration of 10 mM in each drop. Since, there is substantial species selectivity to the inhibition of ALAD by this inhibitor (Kervinen *et al.*, 2001), a high concentration of the inhibitor was used to ensure binding. Crystals of the complex appeared within 3–4 weeks and were flash-cooled in liquid ethane using ~30% (*v/v*) glycerol as a cryoprotectant for cryostorage under liquid nitrogen.

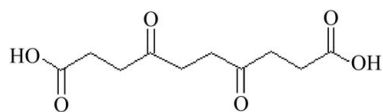


**Figure 2**  
The chemical formula of the diacid ALAD inhibitor 4,7-dioxosebacic acid.

Synchrotron X-ray data sets were collected to 2.6 Å resolution at the ESRF (Grenoble, France) using beamline 14-2 and these were used for the structure determination of the bound inhibitor. The data were processed using the program *MOSFLM* (Leslie, 1992) and were merged using *SCALA* from the *CCP4* suite (Collaborative Computational Project, Number 4, 1994). The data-collection and processing statistics are shown in Table 1. The complexes were non-isomorphous with other crystal forms, so molecular replacement was conducted using the structure of *C. vibrioforme* ALAD (PDB code 1w1z) as the search model using *MOLREP* (Vagin & Teplyakov, 1997) from the *CCP4* suite. The molecular replacement gave a clear solution relating to a dimer in the asymmetric unit. The rotation-function peaks were 7.12 r.m.s. and 6.98 r.m.s. and the highest noise peak was 3.12 r.m.s. The translation function for the first monomer yielded a solution of 51.09 r.m.s., with the next noise peak being at 38.52 r.m.s. For the translation function to locate the second monomer, a solution of 289.46 r.m.s. was found, with the next highest noise peak being at 185.85 r.m.s.

The presence of a bound ligand was determined by calculation of difference Fourier maps using the phases from the native *C. vibrioforme* ALAD structure, as positioned by *MOLREP*. The structure was then refined using *SHELX-97* (Sheldrick, 1998), initially by rigid-body refinement. This was followed by stereochemically restrained least-squares refinement of atomic coordinates and isotropic temperature factors. Subsequent refinements to the structure were carried out using the program *REFMAC* (Murshudov *et al.*, 1997).

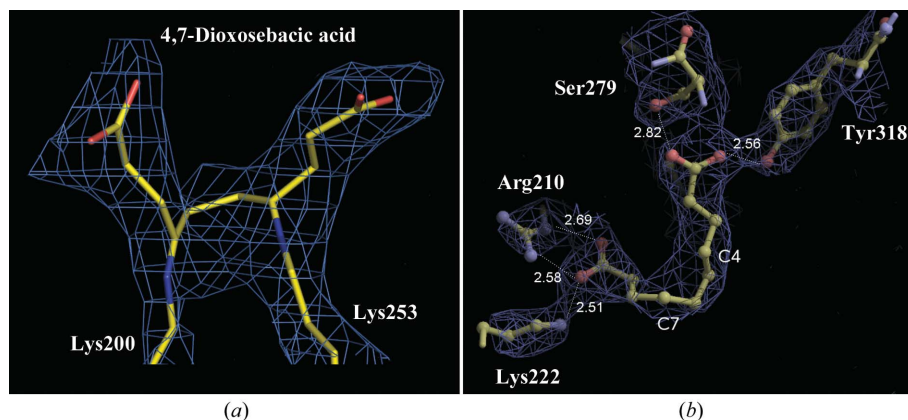


**Figure 3**  
(a) The  $2F_o - F_c$   $\sigma_A$ -weighted electron-density map (shown in cyan) for the inhibitor 4,7-dioxosebacic acid at 2.60 Å resolution. The covalent bonds between the inhibitor and lysines 200 and 253 are also shown. (b) The hydrogen bonds made by the carboxyl groups of the inhibitor with surrounding residues (donor–acceptor distances are shown in Å). The atoms labelled C4 and C7 are attached to the invariant lysine residues by Schiff bases. In both (a) and (b) the map is contoured at 1.25 r.m.s. and the A-site of the enzyme is on the left-hand side, with the P-site on the right.

**Table 1**

X-ray data and refinement statistics for the *C. vibrioforme* ALAD complex.

The space group was  $P4_21_2$ . Values in parentheses are for the outer shell.

Ligand	4,7-Dioxosebacic acid
Unit-cell parameters	
$a = b$ (Å)	126.5
$c$ (Å)	81.6
No. of crystals	1
Resolution range (Å)	89.9–2.6 (2.74–2.60)
$R_{\text{merge}}$ (%)	11.7 (48.4)
Completeness (%)	91.6 (94.1)
Multiplicity	4.0 (4.0)
Mean $I/\sigma(I)$	5.6 (1.60)
Refinement	
$R$ factor (%)	26.0
$R_{\text{free}}$ (%) (5% test set)	32.0
No. of reflections	24586
No. of protein atoms	4964
No. of water atoms	303
No. of ligand atoms	30

Graphical rebuilding was performed using *TURBO-FRODO* (Bio-Graphics, Marseille) running on Silicon Graphics computers using  $\sigma_A$ -weighted maps (Read, 1986). During the model-building process, 303 well ordered water molecules were added to the structure. Various modifications to the restraint dictionaries were made to incorporate the ligand molecules and to ensure planarity of the Schiff bases formed with the enzyme.

### 3. Results

The presence of 4,7-dioxosebacic acid in the crystallization conditions produced a crystal form with a  $c$  axis half that of the native crystal form of *C. vibrioforme* ALAD (Coates *et al.*, 2004). This halved the volume of the unit cell, giving better refinement statistics than the previous structure (PDB code 1w1z), which also had a dimer in the asymmetric unit. The first nine residues of each subunit were not clearly defined by the electron density and so these residues were omitted from the final model. These residues are located at the start of the arm region and are likely to be mobile. Clear electron density for the bound ligand was found at the active site in the initial difference Fourier maps, confirming that binding to the enzyme had occurred. The structure was refined to 2.6 Å resolution and the crystallographic  $R$  factor and free  $R$  factor are given in Table 1 along with other refinement statistics.

The refined structure has 85% of residues within the ‘most favoured’ regions of the Ramachandran plot, with the other 15% being in the additionally allowed regions by the criteria used in *PROCHECK* (Laskowski *et al.*, 1993). The average  $B$  factor for all protein

atoms in the first monomer was  $35.18 \text{ \AA}^2$  and for the second monomer was  $33.38 \text{ \AA}^2$ . The structure and position of the amino acids in and around the active site are conserved between monomers; however, there are slight differences in the conformation of the inhibitor in the two monomers.

The refined electron-density map for the ligand is shown in Fig. 3. All of the 4,7-dioxosebacic acid molecule is reasonably well defined in the electron-density map at  $2.6 \text{ \AA}$  resolution. The absence of disorder in this inhibitor complex may correlate with the ligand's tightly bound state held by two Schiff bases with the enzyme. Studies with substrate 5-aminolaevulinic acid and the inhibitors laevulinic acid, succinylacetone and 4-keto-5-aminohexanoic acid have helped to define the residues forming the P-site (Erskine *et al.*, 1997; Erskine, Newbold *et al.*, 1999; Erskine, Norton *et al.*, 1999, 2001; Frankenberg *et al.*, 1999). Likewise, the ligand in the present study forms a Schiff base with Lys253 and binds with its P-site carboxyl group, making hydrogen bonds with Ser279 and Tyr318. These interactions are characteristic of all other P-site ligands that have been studied previously. These molecules fit in a hydrophobic pocket beneath the active-site flap (205–225) which becomes substantially more ordered when the inhibitors bind. This ordering appears to arise from tight hydrophobic interactions between the P-site ligands and residue Phe209. Kinetic studies on *E. coli* ALAD have suggested that the  $K_M$  of the P-site ( $4.6 \mu\text{M}$ ) is lower than that of the A-site ( $66 \mu\text{M}$ ) (Jarret *et al.*, 2000; Neier, 2000). In consequence, the residues which bind the A-side substrate have been more elusive to define.

Thus, whilst the majority of previous studies defined the enzyme's P-site (see above), the inhibitor used in the present study provides good definition of the A-site residues. The 4,7-dioxosebacic acid also makes a second Schiff base through its C-7 keto function with Lys200, as has been observed in complexes of this inhibitor with yeast and *E. coli* ALAD (Erskine *et al.*, 2001; Kervinen *et al.*, 2001; Jaffe *et al.*, 2002). This was clearly shown by the initial difference electron density and has been confirmed by subsequent refinement at  $2.6 \text{ \AA}$  resolution. The A-site carboxyl group forms a hydrogen bond with the side-chain  $\text{NH}_2$  group of Lys222 ( $2.5 \text{ \AA}$ ) and two hydrogen bonds ( $2.6$ ,  $2.7 \text{ \AA}$ ) with the guanidinium group of Arg210 (Fig. 3). The P-site carboxyl group forms hydrogen bonds with Ser279 ( $2.8 \text{ \AA}$ ) and Tyr318 ( $2.6 \text{ \AA}$ ).

#### 4. Discussion

Most mechanistic proposals for ALAD involve the formation of a Schiff base between the P-side substrate moiety and an active-site lysine (Lys253 in *C. vibrioforme* ALAD). This was first indicated by labelling studies, which showed that only the P-side substrate moiety becomes covalently trapped upon reduction with  $\text{NaBH}_4$  (Gibbs & Jordan, 1986). It is likely that upon binding of the A-side substrate the ensuing reaction with P-side substrate is sufficiently fast to preclude trapping of a Schiff base at the A-site under the conditions used in these earlier studies. The finding that the 4,7-dioxosebacic acid inhibitor forms Schiff bases with both of the invariant active-

site lysine residues (200 and 253 in *C. vibrioforme* ALAD) suggests that both A- and P-side substrate may form Schiff bases upon productive binding to the enzyme. This binding pattern has been shown to occur in the zinc-dependent ALADs (Erskine, Coates *et al.*, 2001; Kervinen *et al.*, 2001) and from this study also appears to be the case in the *C. vibrioforme* zinc-independent ALAD.

The binding interactions of the inhibitor 4,7-dioxosebacic acid with *C. vibrioforme* ALAD were compared with those made by the same compound with yeast ALAD (PDB code 1eb3) and with *E. coli* ALAD (PDB code 1i8j). The binding of the inhibitor to the P-site is similar in all three ALADs (Fig. 4). However, the conformation of the inhibitor in the A-site of the *C. vibrioforme* ALAD differs slightly from that in yeast and *E. coli* ALADs, presumably owing to major differences in this part of the active site. In the yeast and *E. coli* ALADs, the active-site zinc ion is bound by three cysteines and a solvent molecule, which form one side of the A-site against which the inhibitor packs. These ligands could neutralize the charge on the zinc ion. In contrast, the *C. vibrioforme* ALAD active site lacks a zinc ion and two of the cysteines are replaced by aspartates and the other by alanine. Thus, the A-site is probably more polar and is larger as well as being occupied by more water molecules in the *C. vibrioforme* complex. Thus, it is reasonable to expect that the aliphatic part of the inhibitor occupying this pocket would bind less tightly to the *C. vibrioforme* enzyme than to the yeast or *E. coli* enzymes, as has been shown experimentally (Kervinen *et al.*, 2001).

The inhibitor carboxyl in the A-site forms a number of important electrostatic interactions and hydrogen bonds, including one with Lys222. This residue is replaced by an arginine in both the yeast and *E. coli* structures and the arginine side chain also interacts with the inhibitor carboxyl. Lys222 forms an additional hydrogen bond with one of the aspartates (Asp127) that replace the cysteine ligands to the zinc ion present in the yeast and *E. coli* ALADs. Thus, it appears that the substitution of the zinc-binding cysteine (Cys135 in yeast ALAD) with the larger aspartate side chain (Asp127 in *C. vibrioforme* ALAD) requires a compensating

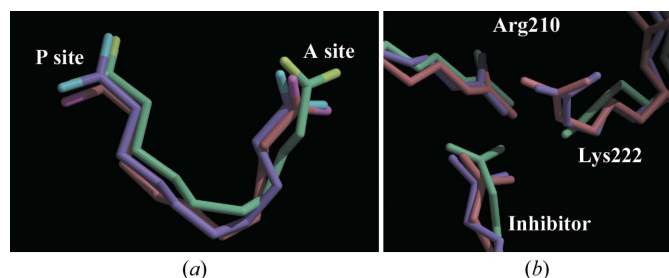


**Figure 4**  
(a) The different conformations the inhibitor 4,7-dioxosebacic acid adopts when binding to different ALADs are shown. The conformation of the inhibitor bound to the *E. coli* enzyme is shown in pink, while that of the yeast enzyme is shown in purple, with the conformation of the inhibitor bound to *C. vibrioforme* ALAD shown in green. (b) The interactions of 4,7-dioxosebacic acid from the three structures with the residues making up the A-site (the colouring scheme remains the same). Lys222 from the *C. vibrioforme* structure is replaced by an arginine residue in both the *E. coli* and yeast ALADs.

substitution of an arginine side chain (Arg232 in yeast ALAD) to a smaller, but still basic, side chain (Lys222) in *C. vibrioforme* ALAD. Thus, the occurrence of arginine at this position is a common feature of the zinc-dependent ALADs and likewise, zinc-independent ALADs show a preference for lysine at the same position.

The A-side carboxyl group of the inhibitor forms similar interactions with a conserved arginine in all three structures (Arg210 in *C. vibrioforme* ALAD). The finding that the inhibitor bound to *C. vibrioforme* ALAD adopts a slightly different conformation in the A-site is probably caused by the occurrence of lysine at position 222 instead of arginine in the other structures and the fact that the A-site of the *C. vibrioforme* ALAD is appreciably larger than in the other two ALADs owing to the lack of a tightly bound zinc ion.

We gratefully acknowledge the financial support of the BBSRC (UK). We also thank the ESRF (Grenoble) for access to synchrotron beam time and associated travel funds. We are indebted to F. Stauffer and R. Neier (Institut de Chimie, Université de Neuchâtel, Switzerland) for kind provision of the inhibitor 4,7-dioxosebacic acid.

## References

- Bollivar, D. W., Clauson, C., Lighthall, R., Forbes, S., Kokona, B., Fairman, R., Kundrat, L. & Jaffe, E. K. (2004). *BMC Biochem.* **5**, 17.
- Breinig, S., Kervinen, J., Stith, L., Wasson, A. S., Fairman, R., Wlodawer, A., Zdanov, A. & Jaffe, E. K. (2003). *Nature Struct. Biol.* **10**, 757–763.
- Brennan, M. J. W. & Cantrill, R. C. (1979). *Nature (London)*, **280**, 514–515.
- Coates, L., Beaven, G., Erskine, P. T., Beale, S., Gill, R., Mohammed, F., Wood, S. P. & Shoolingin-Jordan, P. (2004). *J. Mol. Biol.* **342**, 563–570.
- Collaborative Computational Project, Number 4 (1994). *Acta Cryst. D* **50**, 760–763.
- Doss, M., Von-Tieperman, R., Schneider, J. & Schmid, H. (1979). *Klin. Wochenschr.* **57**, 1123–1127.
- Erskine, P. T., Coates, L., Butler, D., Youell, J., Brindley, A. A., Wood, S. P., Warren, M. J., Shoolingin-Jordan, P. M. & Cooper, J. B. (2003). *Biochem. J.* **373**, 733–738.
- Erskine, P. T., Coates, L., Newbold, R., Brindley, A. A., Stauffer, F., Wood, S. P., Warren, M. J., Cooper, J. B., Shoolingin-Jordan, P. M. & Neier, R. (2001). *FEBS Lett.* **503**, 196–200.
- Erskine, P. T., Newbold, R., Brindley, A. A., Wood, S. P., Shoolingin-Jordan, P. M., Warren, M. J. & Cooper, J. B. (2001). *J. Mol. Biol.* **312**, 133–141.
- Erskine, P. T., Newbold, R., Roper, J., Coker, A., Warren, M. J., Shoolingin-Jordan, P. M., Wood, S. P. & Cooper, J. B. (1999). *Protein Sci.* **8**, 1250–1256.
- Erskine, P. T., Norton, E., Cooper, J. B., Lambert, R., Coker, A., Lewis, G., Spencer, P., Sarwar, M., Wood, S. P., Warren, M. J. & Shoolingin-Jordan, M. J. (1999). *Biochemistry*, **38**, 4266–4276.
- Erskine, P. T., Senior, N., Awan, S., Lambert, R., Lewis, G., Tickle, I. J., Sarwar, M., Spencer, P., Thomas, P., Warren, M. J., Shoolingin-Jordan, P. M., Wood, S. P. & Cooper, J. B. (1997). *Nature Struct. Biol.* **4**, 1025–1031.
- Frankenberg, N., Erskine, P. T., Cooper, J. B., Shoolingin-Jordan, P. M., Jahn, D. & Heinz, D. W. (1999). *J. Mol. Biol.* **289**, 591–602.
- Gibbs, P. N. B. & Jordan, P. M. (1986). *Biochem. J.* **236**, 447–451.
- Jaffe, E. K. (1995). *J. Bioenerg. Biomembr.* **27**, 169–179.
- Jaffe, E. K. (2000). *Acta Cryst. D* **56**, 115–128.
- Jaffe, E. K. (2003). *Chem. Biol.* **10**, 25–34.
- Jaffe, E. K. (2004). *Bioorg. Chem.* **32**, 316–325.
- Jaffe, E. K., Kervinen, J., Martins, J., Stauffer, F., Neier, R., Wlodawer, A. & Zdanov, A. (2002). *J. Biol. Chem.* **277**, 19792–19799.
- Jaffe, E. K., Martins, J., Li, J., Kervinen, J. & Dunbrack, R. L. Jr (2001). *J. Biol. Chem.* **276**, 1531–1537.
- Jarret, C., Babalova, J., Stauffer, F., Henz, M. E. & Neier, R. (1998). *Electronic Conference on Heterocyclic Chemistry 98 (ECHET98)*, edited by H. J. Rzepa & O. Kappe (Editors), Article 103. London: Imperial College Press.
- Jarret, C., Stauffer, F., Henz, M. E., Marty, M., Luond, R. M., Bobalova, J., Schurmann, P. & Neier, R. (2000). *Chem. Biol.* **7**, 185–196.
- Jordan, P. M. (1991). *New Comput. Biochem.* **19**, 1–65.
- Jordan, P. M. (1994). *Curr. Opin. Struct. Mol. Biol.* **4**, 902–911.
- Jordan, P. M. & Gibbs, P. N. B. (1985). *Biochem. J.* **227**, 1015–1020.
- Jordan, P. M. & Seehra, J. S. (1980a). *J. Chem. Soc. Chem. Commun.*, pp. 240–242.
- Jordan, P. M. & Seehra, J. S. (1980b). *FEBS Lett.* **114**, 283–286.
- Kervinen, J., Jaffe, E. K., Stauffer, F., Neier, R., Wlodawer, A. & Zdanov, A. (2001). *Biochemistry*, **40**, 8227–8236.
- Laskowski, R. A., MacArthur, M. W., Moss, D. S. & Thornton, J. M. (1993). *J. Appl. Cryst.* **26**, 283–291.
- Leslie, A. G. W. (1992). *Jnt CCP4/ESF-EAMCB Newsl. Protein Crystallogr.* **26**.
- Mitchell, G., Laroche, J., Lambert, M., Michaud, J., Grenier, A., Ogier, H., Gauthier, M., Lacroix, J., Vanasse, M., Larbrisseau, A., Paradis, K., Weber, A., Lefevre, Y., Melancon, S. & Dallaire, L. (1990). *N. Engl. J. Med.* **322**, 432–437.
- Murshudov, G. N., Vagin, A. A. & Dodson, E. J. (1997). *Acta Cryst. D* **53**, 240–255.
- Neier, R. (2000). *J. Heterocycl. Chem.* **37**, 487–508.
- Read, R. J. (1986). *Acta Cryst. A* **42**, 140–149.
- Senior, N., Thomas, P. G., Cooper, J. B., Wood, S. P., Erskine, P. T., Shoolingin-Jordan, P. M. & Warren, M. J. (1996). *Biochem. J.* **320**, 401–412.
- Sheldrick, G. M. (1998). In *Crystallographic Computing 7*, edited by P. E. Bourne & K. D. Watenpaugh. Oxford University Press.
- Simons, T. J. B. (1995). *Eur. J. Biochem.* **234**, 178–183.
- Stauffer, F., Zizzari, E., Engeloch-Jarret, C., Faurite, J.-P., Babalova, J. & Neier, R. (2001). *ChemBioChem*, **2**, 343–354.
- Vagin, A. & Teplyakov, A. (1997). *J. Appl. Cryst.* **30**, 1022–1025.
- Warren, M. J., Cooper, J. B., Wood, S. P. & Shoolingin-Jordan, P. M. (1998). *Trends Biochem. Sci.* **23**, 217–221.
- Warren, M. J. & Scott, A. I. (1990). *Trends Biochem. Sci.* **15**, 486–491.